

Comparison of Different Ionization Models for a Glow Discharge

Hendrik J. Viljoen

Dept. of Chemical Engineering, University of Nebraska, Lincoln, NE 68588

Dariusz Orlicki and Vladimir Hlavacek

Laboratory for Ceramic and Reaction Engineering, Dept. of Chemical Engineering, State University of New York, Buffalo, NY 14260

Introduction

Plasma reactors have gained prominence as important materials processing tools. Particularly glow discharge reactors have become indispensable in the manufacturing of electronic parts, since their introduction in the mid 60s. A strong motivation for modeling these reactors is that the system is highly nonlinear and sensitive to small changes in design and operating variables, perturbations and intrusions in the plasma space. The parameter space is large and the optimization of a system requires a numerical model to simulate the process.

The film that is grown in a glow discharge process depends strongly on the nature of the discharge itself. Therefore, it is important to model the discharge *per se* in sufficient detail. Before "sufficient" is quantified, it is necessary to look at different approaches to model the discharge. Macroscopic approaches rely on energy-averaged moments of the Boltzmann equation to describe the position dependency of variables in the gap. These models can capture most of the qualitative features of the discharge. Microscopic approaches are computationally more expensive, but information about the energy distribution of the charged species is obtained. The latter approach permits a more accurate calculation of reaction rates for radical formation. If the purpose of the model is to get a qualitative understanding of the film deposition, a macroscopic approach could suffice, but for quantitative modeling, a microscopic approach is necessary. In a recent note, Gustafson et al. (1990) addressed the importance of the electron energy distribution function on the reaction kinetics.

A number of different macroscopic models have been developed to describe ionization. Microscopic models all originate from the Boltzmann equation, and different assumptions and simplifications determine the sophistication of each model. In this note, the ionization rate of Ar in a DC glow discharge will be calculated by different models. The electric field will be an input that is, nonself-consistent, and models will be

compared for the same electric field. In Figure 1, the electric field is shown. It has the typical form of an electric field in a DC glow discharge; with a strong component near the cathode, a sign reversal and relatively small (and constant) value in the bulk of the domain and near the anode it decreases once again.

Macroscopic Models

The form of rate expression that will be used for comparison is the Townsend coefficient α , which is defined as:

$$\frac{dJ}{dx} = \alpha J$$

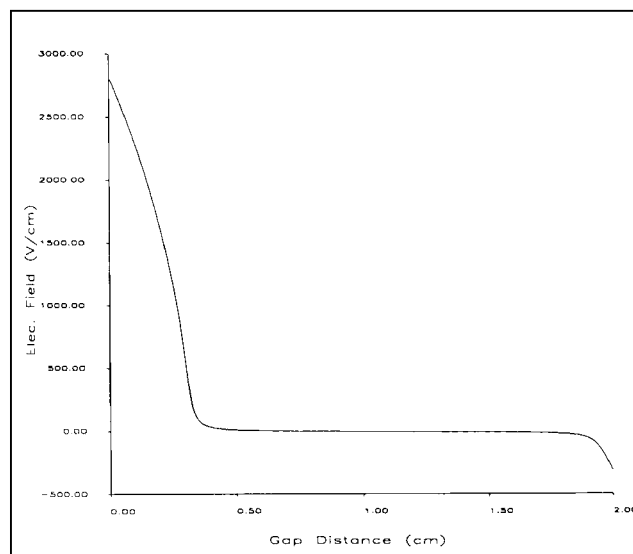


Figure 1. Electric field.

Correspondence concerning this work should be addressed to H. J. Viljoen.

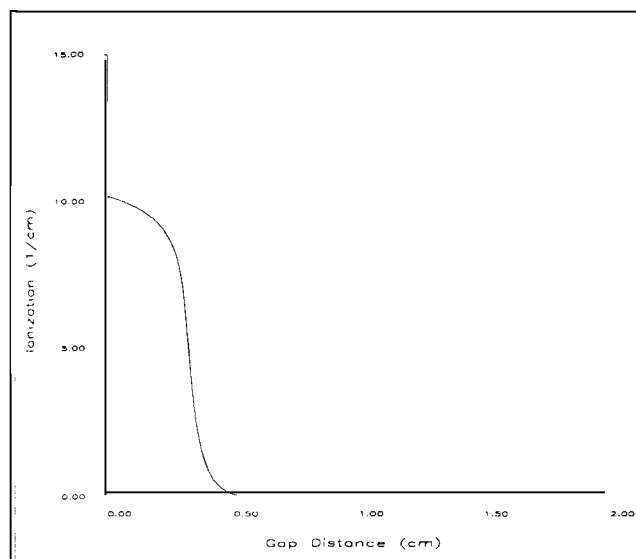


Figure 2. Ionization coefficient for equilibrium model.

where J is the electron flux. In more conventional terms, the rate could be expressed as the product of electron concentration and a rate constant k_e (unit of 1/time) and $k_e = \alpha W$, where W denotes a local drift velocity.

If it is assumed that the electron cloud is in equilibrium with the electric field at each point in space, the following expression can be used for calculating the Townsend ionization coefficient:

$$\alpha_{eq}(x) = A P e^{-B/[E(x)/P]^r} \quad (1)$$

Constants A and B are readily available for a wide range of gases (Nasser, 1966). For Ar, the values $A = 13.6$ (1/cm·torr) and $B = 235$ have been used to calculate α_{eq} and the pressure P was 1 torr. Constant r usually has the value of 1/2. In Eq. 1, the units of pressure and electric field are torr and V/cm. Figure 2 shows the results of α_{eq} . Equation 1 is defined only for $E(x) > 0$ and $\alpha_{eq} \rightarrow 0$ when $E(x) \rightarrow 0^+$. Once $E(x)$ has changed sign, α_{eq} is kept zero. Ionization is limited to the cathodic sheath, as expected, but what sets this result aside from other models is the maximum at the cathode, which results from the equilibrium that exists with the electric field and Eq. 1 has a maximum at the cathode.

Nonequilibrium models are more realistic, and the influence of the electric field prior to the point x on the ionization coefficient $\alpha(x)$ is taken in consideration. We will look at two nonequilibrium macroscopic models. The first one was proposed by Segur et al. (1982). This model retains the functional form of α as defined by Eq. 1, but instead of $E(x)$, an effective electric field is used. $E_{eff}(x)$ is defined as follows:

$$E_{eff} = \int_0^x E(x') \phi(x-x') dx' \quad (2)$$

and the "memory factor" function ϕ has been determined from greatly simplified physical considerations and a large number of Monte Carlo simulations. Segur et al. (1982) proposed the following form for ϕ :

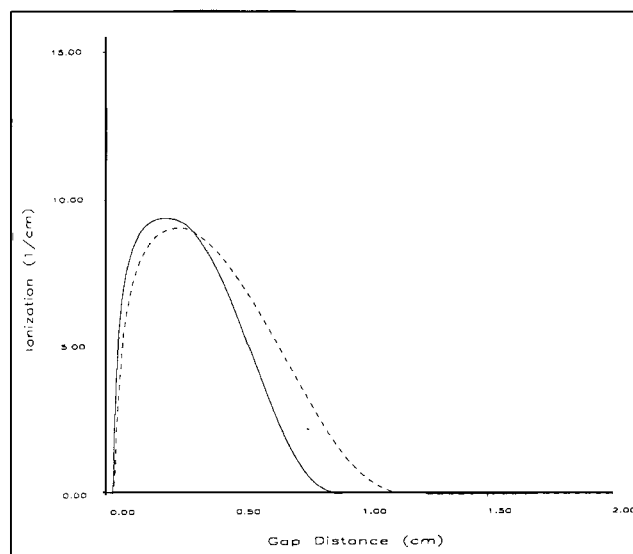


Figure 3. Ionization coefficient for Segur's model.

$\lambda = 0.1$ cm (—); $\lambda = 0.15$ (---).

$$\phi(x) = \frac{2}{\lambda} e^{-x/\lambda} (1 - e^{-x/\lambda}) \quad (3)$$

where λ is a parameter that is unique for each gas or gaseous system. Note that in Segur et al.'s article, ϕ was incorrectly defined. They found that for a value of $\lambda = 0.15$ cm for He, the Townsend coefficient α_{mf} correlated best with values calculated by the Monte Carlo method. Unfortunately no values were reported for any other gases. In Figure 3, α_{mf} is shown for $\lambda = 0.15$ cm and $\lambda = 0.1$ cm. An increase in λ decreases the maximum and shifts it away from the cathode. Overall, it tends to distribute the ionization more through the gap. A smaller λ has the opposite effect, and the ionization coefficient has a sharper and higher peak closer to the cathode.

The second macroscopic model was proposed by Friedland (1974), but in a later article (Friedland and Kagan, 1985), a better derivation of the equation was given. A forward-scattering model is used and it is also assumed that the ionization and excitation collision cross-sections are linear functions of the electron energy (ϵ):

$$Q_i = a\epsilon$$

$$Q_e = k\epsilon$$

For Ar, the values of a and k were reported as 0.53 and 0.21 (cm·torr·eV)⁻¹, respectively. The one-space, one-velocity component form of the Boltzmann equation (forward scattering model) is considered. By taking the first and second moments with respect to ϵ , two closed equations are obtained, which are the electron flux (J) and electron energy flux ($\bar{\epsilon}$) balances, respectively:

$$\frac{dJ}{dx} = Pa\bar{\epsilon} \quad (4)$$

$$\frac{d\bar{\epsilon}}{dx} = E(x)J - P(\epsilon_1 k + \epsilon_2 a)\bar{\epsilon} \quad (5)$$

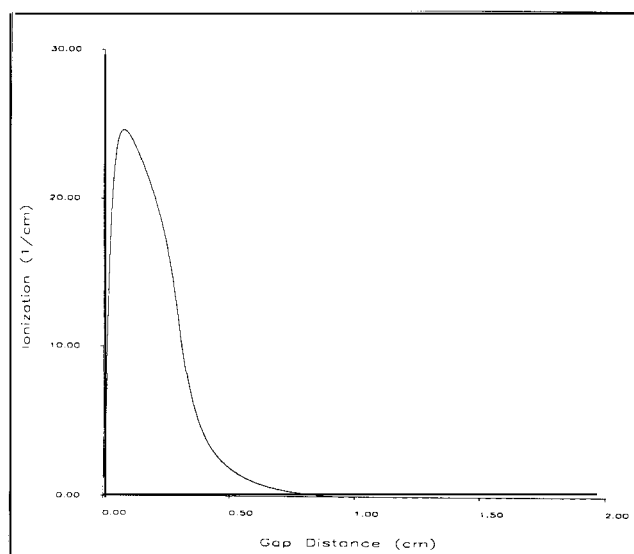


Figure 4. Ionization coefficient for Friedland's model.

Using the definition for the Townsend coefficient, the following nonlinear first-order equation is obtained from Eqs. 4 and 5:

$$\frac{d\alpha_F}{dx} + \alpha_F^2 + P(\epsilon_1 k + \epsilon_2 a)\alpha_F - PaE(x) = 0 \quad (6)$$

with the initial condition $\alpha_F = 0$ at the cathode. The threshold values for ionization and excitation were taken as $\epsilon_2 = 15.7$ eV and $\epsilon_1 = 11.5$ eV, respectively. Friedland and Kagan (1985) also used quadratic forms for the collision cross-sections, but the model required additional assumptions for closure and it fails when electron energies become too large (the cutoff can be associated with the energy where the quadratic form becomes negative). In Figure 4, α_F is shown, using the electric field of Figure 1.

Another macroscopic approach to model the discharge is based on the electron temperature. Assuming a form for the electron energy distribution, one can define an electron temperature and species and temperature balances can be derived. The ionization rate takes the form of an irreversible first-order chemical reaction with Arrhenius kinetics and it depends on both electron temperature and electron concentration distributions in the gap. To make a comparison, further assumptions regarding the fluid-like properties of the charged species must be made, transport parameters must be known, boundary conditions must be formulated, and the conservation equations must be solved. A fair comparison can be made only if the governing equations are also solved for the ionization models considered, but it falls outside the scope of this note.

Microscopic Model

The microscopic model that we will use is known as the multibeam model, and it can be derived from the Boltzmann equation, again for the special case of forward scattering only. Carman and Maitland (1987) and Carman (1989) used this model to calculate the electron flux energy distribution

(EFEDF) for the cathode fall region of He and Ar discharges, but a better exposition of the model is given by Surendra et al. (1990).

The electron flux (EFEDF) is considered a function of both position and energy. In discrete form, the solution space consists of cells which measure $1 \text{ eV} \times dx$ and a cell located at (x, ϵ) is populated by $\text{EFEDF}(x, \epsilon) \times 1 \text{ eV}$ electrons/ $\text{m}^2 \cdot \text{s}$. When this flux component within an interval is translated by a distance dx , it is redistributed over all the energy intervals at the new spatial position $x + dx$. The energy gained/lost from the electric field during this displacement is $E(x)dx$, but a further redistribution along the energy axis is determined by inelastic collisions. The inelastic collisions consist of ionization and excitation processes, and the frequency of any specific process is given by the ratio of its collision cross-section to the total inelastic cross-section. This way the number of new-born electrons can be easily determined. These new electrons will also occupy the energy space at the position $x + dx$ according to the energy transfer distribution during an ionization collision. Upon collision, the minimum amount of energy that can be transferred from the ionizing electron is the ionization threshold value, leaving the new electron with zero initial energy. Additional energy transfer will increase the initial energy of the ionized electron. For more information about the probability distribution of energy transfer, interested readers are referred to the work of Surendra et al. (1990).

These authors used this model to calculate the energy distribution of that fraction of the electron population which has energy above the minimum inelastic collision threshold: that is, energy axis started at the smallest inelastic threshold value. The model was applied in the cathode fall, negative glow and anodic fall regions of a DC glow discharge. The rate of new-born slow electrons was determined and used in a fluid model for all electrons with energy less than the minimum threshold value to find the total electron distribution. A similar fluid model was used to determine the ion distribution, and the electric field was defined by the Poisson equation.

In criticism of this model, one first notes that the fluid model contains only dependent variables which are averaged over energy space. Subsequently, no information about the energy distribution of the slow electrons is known, except when additional assumptions are made. Hence, it is not possible to calculate the flow of electrons from the slow fraction of the population into the high energy regime. The existence of such a flow is obvious from the fact that ionization occurs throughout the discharge gap, also in the domain where $E(x)$ is negative. Slow new-born electrons that are formed near the anode, for example, will be accelerated toward the cathode; if the plasma potential is sufficiently high, further ionization is possible. Starting near the anode with the part of the flux component that has too little energy to reach the anode, a second solution of the multibeam model is found by integrating toward the cathode. The important point from a mathematical perspective is that the Boltzmann equation is linear (that is, no electron-electron or electron-ion interaction) and different solutions can be added to get the total ionization rate and electron flux distribution.

To treat the feedback from the slow electron population, we propose the following approach. All collision processes are still taken as perfectly forward-scattering (although this assumption becomes poorer as the electron energy is lower) and

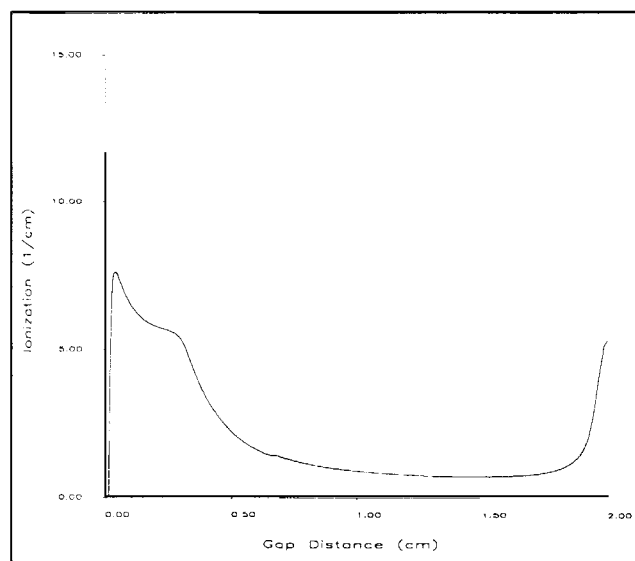


Figure 5. Ionization coefficient for microscopic model (α_{cai}).

the multibeam method is employed for all electrons. For a given electric field $E(x)$, the total electron flux at position x :

$$J(x) = \int_{\epsilon_{\min}}^{\infty} j(x, \epsilon) d\epsilon \quad (7)$$

is the algebraic sum of the “cathode-to-anode” and “anode-to-cathode” elements, $J(x) = [J_{ca}(x) - J_{ac}(x)]$. Each of these elements can be written as a sum:

$$J_{ca}(x) = \sum_0^N J_{cai}(x) \quad (8)$$

and likewise for J_{ac} . Starting with an initial distribution at the cathode, J_{ca1} is calculated by the multibeam model. Then, the procedure is repeated from the anode, starting next to the anode with the flux of electrons that has energy too low to reach the anode, since they will be accelerated toward the cathode. In this sweep, J_{ac1} is calculated. Off-spring of this first generation flux will determine the starting conditions for the next sweep toward the anode. The ionization rate associated with each sweep forms a convergent series, since higher flux components ($i > 1$) will be accelerated from levels that are closer to the plasma potential. In this sense, the plasma potential acts like a potential well.

The collision cross-sections used in this study were reported by Vicek (1989). We also did not put the restriction on the model that $E(x)dx$ must be integer-valued. When the energy at the new position for each process (no-collision, ionization, excitation) was calculated, the flux was distributed between the two adjacent intervals to maintain the average energy. For example, a flux will be distributed in the ratio 0.4:0.6 between the 4 eV and 3 eV intervals for an energy of 3.4 eV. The Townsend coefficients associated with each flux component J_{cai} or J_{aci} can be calculated. In Figure 5, the ionization coefficient for the first cathode to anode flux, J_{ca1} is shown. The

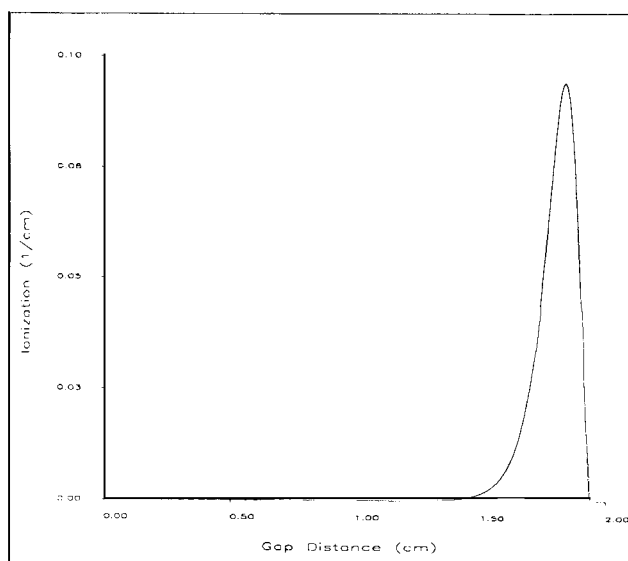


Figure 6. Ionization coefficient for microscopic model (α_{ac1}).

coefficient associated with J_{ca1} is, of course, the same as the one calculated by the conventional multibeam model. Note the increase in α closer to the anode. This can be easily explained, keeping the definition of α in mind. The total flux flowing toward the anode decreases, because the opposing electric field becomes stronger, while the high energy electrons continue to ionize Ar atoms. In Figure 6, α_{ac1} is shown (first cathode to anode sweep); note the scales of Figures 5 and 6, which show that α_{ca1} is almost two orders of magnitude larger than α_{ac1} , affirming the convergence property.

Discussion

When the results for the different macroscopic models are compared with each other, several points come to mind. First, one notes that with the exception of the Friedland model, the maximum value of the ionization coefficient is very consistent (8–10/cm). The Friedland model overestimates the maximum by the factor of three, and it is a consequence of the assumption that the inelastic cross-sections depend linearly on electron energy. As far as the distribution of the ionization coefficient in space is concerned, the Friedland model and equilibrium model predict a ionization in the first 25% of the gap, but Segur's model predicts ionization in 50% of the gap. These differences will reflect in the mean electron energy distribution (this distribution is important for macroscopic models, since it is used to compute rate constants for radical formation), and differences in radical concentration and distribution can be expected for the different models.

The microscopic model used has multiple ionization coefficients. The first one (α_{ca1}) has a maximum of 7.6/cm, which is in good agreement with the macroscopic model of Segur (maxima are 9.0 and 9.4 for $\lambda = 0.15$ cm and 0.1 cm, respectively). α_{ac1} is much smaller, with a maximum of approximately 0.1/cm. This term is associated with the potential drop near the anode and a higher plasma potential will reflect in a larger second ionization term. Taking α_{ca1} as our yardstick, one can conclude that of all the macroscopic models considered, Segur's model compares the best with the microscopic model.

Notation

a = coefficient in Eq. 4, $1/\text{cm} \cdot \text{torr} \cdot \text{eV}$
 A = coefficient in Eq. 1, $1/\text{cm} \cdot \text{torr}$
 B = coefficient in Eq. 1
 E = electric field, V/cm
 j = distributed (in energy and space) electron flux, $1/\text{cm}^2 \cdot \text{s} \cdot \text{eV}$
 J = energy-averaged electron flux, $1/\text{cm}^2 \cdot \text{s}$
 k = coefficient in Eq. 4, $1/\text{cm} \cdot \text{torr} \cdot \text{eV}$
 k_e = ionization rate constant, $1/\text{s}$
 P = pressure in gap, torr
 Q_e = excitation cross-section, cm^2
 Q_i = ionization cross-section, cm^2
 W = drift velocity, cm/s
 x = distance from cathode, cm

Greek letters

α = Townsend ionization coefficient, $1/\text{cm}$
 ϵ = electron energy, eV
 $\bar{\epsilon}$ = mean energy flux, $\text{eV/cm}^2 \cdot \text{s}$
 ϕ = memory function, defined by Eq. 3
 λ = parameter in Segur's model, see Eq. 3, cm

Subscripts

1 = average excitation threshold
2 = ionization threshold
eq = equilibrium model

F = Friedland model
 mf = memory factor model

Literature Cited

- Carman, R. J., "A Simulation of Electron Motion in the Cathode Sheath Region of a Glow Discharge in Argon," *J. Phys. D: Appl. Phys.*, **22**, 55 (1989).
Carman, R. J., and A. Maitland, "Electron Behavior in a Helium Glow Discharge," *J. Phys. D: Appl. Phys.*, **20**, 1021 (1987).
Friedland, L., "Electron Multiplication in a Gas Discharge at High Values of E/P ," *J. Phys. D: Appl. Phys.*, **7**, 2246 (1974).
Friedland, L., and Yu M. Kagan, "Reduced Kinetic Description of Electron Multiplication in Gases," *J. Phys. D: Appl. Phys.*, **19**, 1019 (1986).
Gustafson, J. B., A. N. Beris, and H. C. Foley, "Reaction Phenomena in a Nonthermal Equilibrium Plasma," *AIChE J.*, **36**, 1439 (1990).
Nasser, E., *Glow Discharge Processes*, Wiley, New York (1966).
Segur, P., M. Yousfi, J. P. Boeuf, E. Marode, A. J. Davies, and J. G. Evans, "The Microscopic Treatment of Nonequilibrium Regions in a Weakly Ionized Gas," *Proc. Conf. on Plasma* (1982).
Surendra, M., D. B. Graves, and G. M. Jellum, "Self-Consistent Model of a Direct-Current Glow Discharge: Treatment of Fast Electrons," *Phys. Rev. A*, **41**, 1112 (1990).
Vicek, J., "A Collisional-Radiative Model Applicable to Argon Discharges Over a Wide Range of Conditions: Formulation and Basic Data," *J. Phys. D: Appl. Phys.*, **22**, 623 (1989).

Manuscript received Feb. 6, 1992, and revision received June 16, 1992.